

Electron coherent and incoherent pairing instabilities in inhomogeneous bipartite and nonbipartite nanoclusters

A. N. Kocharian

*Department of Physics, California State University,
Los Angeles, CA 90032, USA; Physical Sciences,
Santa Monica College, Santa Monica, CA 90405, USA*

G. W. Fernando and K. Palandage

Department of Physics, University of Connecticut, Storrs, CT 06269, USA

J. W. Davenport

Computational Science Center, Brookhaven National Laboratory, Upton, NY 11973, USA

Exact calculations of collective excitations and charge/spin (pseudo)gaps in an ensemble of bipartite and nonbipartite clusters yield level crossing degeneracies, spin-charge separation, condensation and recombination of electron charge and spin, driven by interaction strength, inter-site couplings and temperature. Near crossing degeneracies, the electron configurations of the lowest energies control the physics of electronic pairing, phase separation and magnetic transitions. Rigorous conditions are found for the smooth and dramatic phase transitions with competing stable and unstable inhomogeneities. Condensation of electron charge and spin degrees at various temperatures offers a new mechanism of pairing and a possible route to superconductivity in inhomogeneous systems, different from the BCS scenario. Small bipartite and frustrated clusters exhibit charge and spin inhomogeneities in many respects typical for nano and heterostructured materials. The calculated phase diagrams in various geometries may be linked to atomic scale experiments in high T_c cuprates, manganites and other concentrated transition metal oxides.

PACS numbers: 65.80.+n, 73.22.-f, 71.10.Fd, 71.27.+a, 71.30.+h, 74.20.Mn

I. INTRODUCTION

Strongly correlated electrons in cuprates, manganites and other transition metal oxides exhibit high T_c superconductivity, magnetism and ferroelectricity accompanied by spatial inhomogeneities at the nanoscale level [1, 2, 3, 4, 5, 6, 7, 8]. Over the past few years there is an increase in interest to electron instabilities in nanoclusters, assembled clusters of correlated materials in various topologies for synthesizing new nanomaterials with unique electronic and magnetic properties [9, 10]. Obviously, there is a clear need for an accurate analysis of electron correlations, fluctuations and instabilities in nanoclusters and large complex systems with competing phases. The closed form solution, existing in the Bethe ansatz ground state [11], is difficult to analyze at finite temperatures $T > 0$ without having to resort to various approximations. Perturbation theory is usually inadequate while numerical methods have serious limitations, such as in the Quantum Monte Carlo method with its notorious sign problem where the resulting approximations often lead to some controversy. On the contrary, exact calculations in small clusters [12, 13, 14, 15, 16] give an appealing alternative for the detection of possible phase separations and spatial inhomogeneities especially at finite temperatures. As far as the authors are aware, an exact analysis of level crossing instabilities (degeneracies) in canonical ground state eigenvalues and corresponding competing average energies at finite temperature for a general on-site interaction U and electron concentra-

tions have not been attempted in small or moderate size clusters [17]. Exact computations of electron instabilities in various cluster geometries at the nanoscale level can be vital to the understanding of the role of thermal and quantum fluctuations for large pairing gaps and a transition temperature T_c in the correlated nanoclusters, nanomaterials and corresponding “large” inhomogeneous systems [18, 19, 20, 21, 22, 23, 24, 25].

Although our approach for “large” systems is only approximate, this class of clusters in an ensemble displays a common behavior which we believe is generic for large thermodynamic systems. Our results for typical bipartite and frustrated (nonbipartite) cluster geometries have successfully mapped out scenarios where many body local effects are sufficient to describe spin-charge separation and pairing pseudogaps at the nanoscale level. Spatial microscopic inhomogeneities have been observed in a number of scanning tunnelling microscopy (STM) probes in doped high- T_c superconductors (HTSCs). There is growing evidence suggesting that inhomogeneities at the nanoscale level, in the so-called stripes surrounded by essentially neutral correlated MH-like antiferromagnetic insulators [26, 27], play a defining role for the electron pairing and the origin of superconductivity at the atomic scale in HTSCs [28, 29]. Besides the existence of charge pairing, the inhomogeneities of possible electronic nature can exist in a form of spatially separated magnetic phases in cuprates and manganites under doping [30]. The magnetic inhomogeneities seen in other transition metal oxides at the nanoscale level, widely discussed in the lit-

erature [31, 32, 33, 34, 35], can be crucial for the spin pairing instabilities, origin of ferromagnetism and ferroelectricity in the spin and charge subsystems [36, 37]. A phase separation of the ferromagnetic clusters embedded in an insulating matrix is believed to be essential to the colossal magnetoresistance (CMR) in manganese oxides. At sufficiently low temperatures, the spin redistribution in an ensemble of clusters can produce inhomogeneities in the ground state and at finite temperatures [24]. The non-monotonous behavior of the chemical potential versus electron concentration found in generalized self consistent approximation [38] also suggests possible electron instabilities and inhomogeneities near half filling. From this perspective, exact studies at $T \geq 0$ of electron charge and spin instabilities at various $U \geq 0$, inter-site couplings and various cluster topologies can give important clues for understanding of charge/spin inhomogeneities and local deformations for the mechanism of pairings and magnetism in “large” concentrated systems whenever correlations are local.

It is a generally believed that a strong on-site Coulomb interaction supports ferromagnetism and is detrimental for the electron pairing and superconductivity in clusters and “large” concentrated systems [39]. Our exact studies of gaps and pseudogaps in finite-size systems have uncovered some important answers related to spin-charge separation, pairing and thermal condensation of the electron charge and spin. Despite this, there is still a vast amount of uncertainties that need to be unravelled: (i) What are the conditions for the electron phase separation instabilities and spin/charge inhomogeneities? (ii) What is the role of inhomogeneities and are these spatial spin/charge *inhomogeneities* crucial for the pairing mechanisms in these compounds? (iii) When treated exactly, what essential features can the Hubbard clusters capture that share similar properties with the “large” concentrated transition metal oxides?

A redistribution of excess electron/hole inhomogeneities or spin up/spin down domains in an ensemble of tetrahedrons for all $U > 0$ depends on the sign of the hopping term [24]. Here we show that in the distorted square pyramids in the perovskite structures, the inter-site coupling c between the apex site with the base can be beneficial or detrimental for the electron pairing or ferromagnetism. An unstable “saturated ferromagnetism”, existing in frustrated lattices at low temperatures and large U for a particular sign of hopping ($t > 0$) [36], implies either antiferromagnetism, unsaturated ferromagnetism, or electron coherent pairing for charge and spin pairing (pseudo)gaps. Here it is argued that for one hole off half filling electrons undergo separate thermal condensation of the charge and spin degrees (independent of cluster topology); the system may be divided into two coexisting and dynamically bound bosonic subsystems, where two types of individual bosonic pairs, made up of double electron charges and oppositely oriented (antiparallel) spins, can fluctuate. We shall see that the phase diagram, under some circumstances, is mostly controlled

by the changes in the cluster geometry (topology).

II. MODEL AND FORMALISM

It is possible to assume that the electron pairing and magnetic instabilities of the purely electronic nature is described by a local Coulomb interaction U in a single band Hubbard model

$$H = -t \sum_{\langle i, j \rangle, \sigma} c_{i\sigma}^\dagger c_{j\sigma} + U \sum_i c_{i\uparrow}^\dagger c_{i\downarrow}^\dagger c_{i\downarrow} c_{i\uparrow} \quad (1)$$

The sign of the hopping amplitude t between the nearest neighbor sites in (1) leads to essential changes of electronic structure. In nonbipartite clusters, such as tetrahedron, we consider $t = \pm 1$. In addition, for the distorted pyramid we take the coupling parameter between the apical site and the atoms in the base equal to ct , with $c \leq 1$. Our studies of the quantum and thermal fluctuations of electrons in finite clusters are based on exact diagonalization, analytical and numerical calculations of energy levels and expressions for the canonical and grand canonical partition functions in various cluster geometries. The exact grand canonical potential Ω_U for the interacting electrons (U) in an external magnetic field (h) is

$$\Omega_U = -T \ln \sum_n e^{-\frac{E_n - \mu N_n - h s_n^z}{T}}, \quad (2)$$

where N and s^z are the number of particles and the projection of the spin in the n -th quantum state. The first and second order responses of the charge and spin degrees due to the changes in the chemical potential μ (doping) or an applied magnetic field are calculated without taking the thermodynamic limit. The competing energy states, in conjunction with the canonical and the grand canonical ensemble, yield valuable insight into electron instabilities in the real nanoclusters and nanomaterials with the correlated electrons. The introduced formalism allows us to describe the smooth and sharp phase transitions with competing stable and unstable inhomogeneities in the canonical and grand canonical ensembles.

Below in Sec. III we provide a detailed description of the general methodology: we define the criteria for the charge and the spin pairing instabilities in the canonical and grand canonical ensembles; formulate the conditions for existence of quantum critical points, coherent pairings and spontaneous transitions in the ground state and corresponding critical temperatures of crossovers for various phases and boundaries in the phase diagrams discussed in Secs. IV and V.

III. GENERAL METHODOLOGY

A. Canonical charge and spin gaps

To facilitate the comparison with the frustrated clusters, we summarize here the main results in the ground state and at the finite temperatures for bipartite and non-bipartite clusters obtained earlier in Refs. [19, 20, 21, 22, 23, 24, 25]. The degrees of freedom for charge and spin, electron and spin pairings, temperature crossovers, quantum critical points, etc. were extracted directly from the thermodynamics of these clusters. One can classify the charge and spin order parameters as an energy difference between the various competing phases by analogy with phase transitions in the thermodynamic limit. In the ground state, the calculated differences in the canonical energy levels between configurations with various numbers of electron charge and spin determine the energy gaps for electron charge and spin excitations. Using the exact partition function in the canonical ensemble, we also analyzed analytical expressions for the average energies for various number of electrons N . For given temperature T and U , we calculated the energy differences $\mu_+ = E(N+1) - E(N)$ and $\mu_- = E(N) - E(N-1)$ for the average canonical energies $E(N)$ by adding or subtracting one electron (charge) in the cluster for a given spin S . The energy difference between the two consecutive excitation energies by adding or subtracting electron can serve as a natural order parameter in a canonical approach. Then the charge gap at finite temperature can be written as $\Delta^c(T) = \mu_+ - \mu_- = E(N+1) + E(N-1) - 2E(N)$. The opening of the gap is a local correlation effect, and clearly does not follow from long range order, as exemplified here. The difference $\mu_+ - \mu_-$ is somewhat similar to the difference $I - A$ for a cluster, where I is the ionization potential and A the electron affinity. For a single “impurity” at half filling and $T = 0$, $I - A$ is equal to U , which represents a screened local parameter U in the Hubbard model [40] (1). Thus the gap picture is analogous to an inter-configuration energy gap for the crossover between different many body ground state ionic configurations in solids. For example, the charge gap is simply equivalent to the energy of the “reaction” between different cluster configurations (d) at fixed N

$$d^N + d^N \rightarrow d^{N+1} + d^{N-1}, \quad (3)$$

i.e., the difference in the canonical energies of ionization and affinity for many body cluster configurations in ensemble. However, the configurational change in the ensemble of isolated clusters is supposedly due to the possible spontaneous fluctuations in the electron numbers and electron redistribution via a charge reservoir. The negative spin gap in the canonical ensemble can be treated correspondingly. We calculate a spin gap as the difference in the average energies between the two cluster configurations with various spin S states, $\Delta^s(T) = E(S+1) - E(S)$, for $E(S)$ being respectively the average canonical energy in the spin sector at fixed N [11].

B. Charge and spin instabilities

Many phenomena and phase transitions invoked in the approximate treatments of “large” concentrated systems are seen also in the exact analysis of pairing instabilities in the canonical ensemble of the small clusters in thermodynamic equilibrium [19, 20, 21, 22, 23, 24, 25]. As we shall see, in some circumstances, small changes of the external parameters can lead to level crossing instabilities in various electron configurations with the formation of negative charge and spin gaps. Physically, a positive gap manifests the phase stability and smooth crossover, while a negative gap describes spontaneous transitions from one stationary state to another. Instead of a full phase separation at $\Delta^{c,s} < 0$, the local inhomogeneities in the clusters can provoke electron redistribution and quantum mixing of the various charge and spin configurations. In the presence of a negative gap, the many-body ground state has an appreciable probability of being found in either of these competing configurations. The collective particle excitations are also reflected in the fluctuations of the pair density in Eq. (3). It is intriguing that these fluctuations make the pair redistribution across the clusters possible even without direct contact between the clusters. These fluctuations play a crucial role of the pair transitions in the absence of electron hopping between clusters in Eq. (1). Near ground state degeneracies, the lowest energy states control the low energy dynamics of the electronic and magnetic transitions over a significant portion of the phase diagram.

The possible quantum critical points, phase transitions and nonzero temperature crossovers are described using a simple cluster approach: we define critical parameters for the level crossing degeneracies or quantum critical points from the vanishing conditions for the canonical charge and spin gaps, *i.e.*, $\Delta^{c,s}(U, c) = 0$. The sign of the gap is also important in identifying the regions for the electron charge and spin instabilities, such as the electron-electron $\Delta^c < 0$, electron-hole $\Delta^c > 0$ pairings in the charge sector or the parallel $\Delta^s < 0$ and opposite $\Delta^s > 0$ spin pairings in the spin sector. The key question here is the exact relationship between the canonical charge Δ^c gap and its corresponding grand canonical spin Δ^s counterpart calculated for various bipartite and frustrated cluster topologies. For charge degrees the negative sign of gap implies phase (charge) separation (*i.e.*, *segregation*) of the clusters into hole-rich (charge neutral) and hole-poor regions. The quantum mixing of the closely degenerate, hole-poor d^{N-1} and hole-rich d^{N+1} clusters for one hole off half filling, instead of causing global phase separation, provides a stable spatial inhomogeneous medium that allows the pair charge to fluctuate. The inhomogeneities favored by the negative gaps are essential for providing the spontaneous redistribution of the electron charge or spin. The inhomogeneities in the charge redistribution for $\Delta^c < 0$ and $\Delta^s = 0$ imply static heterostructure for different electron configurations, close in energy, in an unstable ensemble of clusters. These inhomogeneities

are consistent with nucleation of the “negative” charge gap in cuprates above T_c [6]. At low temperatures, the dynamic picture for pair fluctuations between different electron configurations $\Delta^c < 0$ and $\Delta^s > 0$ is possible at relatively low temperatures in spatially inhomogeneous coherent state ($\Delta^s \equiv -\Delta^c$, see also Sec. IV A). This result is consistent with the observation of nonlocal superconductivity at low excitation energies and at higher energies, holes localized in an inhomogeneous “stripe” pattern [1]. The negative spin gap describes the possible parallel spin pair binding instability. This picture implies spontaneous ferromagnetism and phase (spin) separation into domains in accordance with the Nagaoka theorem. For the negative gaps, one can introduce the critical temperatures $T_c^P(\mu)$ and $T_s^F(\mu)$ versus chemical potential for boundaries between various phases derived from the condition that the corresponding gaps disappear, i.e., $\Delta^{c,s}(T, \mu) = 0$.

C. Charge and spin susceptibility peaks

Conventional phase transitions at finite temperature are driven by thermal fluctuations. In the grand canonical approach using exact analytical expressions for the grand canonical potential and partition functions as expressed in Eq. (2), we have analyzed (in Refs. [19, 20, 21, 22, 23, 24, 25]) the variation of the charge, $\frac{\partial N}{\partial \mu}$, and spin, $\frac{\partial s}{\partial h}$, density of states or corresponding charge $\chi_c(\mu)$ and spin $\chi_s(\mu)$ susceptibilities,

$$\chi_c = \frac{\partial \langle N \rangle}{\partial \mu}, \quad \chi_s = \frac{\partial \langle s^z \rangle}{\partial h} \quad (4)$$

as a function of the chemical potential μ and h in a wide range of temperatures. In a grand canonical approach the energy difference between the two consecutive susceptibility peaks in terms of μ and h at finite temperatures can serve as a natural order parameters for charge and spin degrees respectively. This energy difference for density of states in μ space determines the charge gap in canonical approach. We find (opposite) spin pairing gap by calculating the minimal magnetic field necessary to overturn the spin. In the grand canonical method we define the gap as a magnetic field at which the distance between the subsequent spin susceptibility peaks in μ space vanishes. Using the maxima of zero magnetic field susceptibility, $\frac{\partial s}{\partial h}|_{h \rightarrow 0}$, we also calculated the boundary curve for the onset of the spin gap for various μ in infinitesimal $h \rightarrow 0$ above T_s^P . To distinguish this from the canonical and grand canonical gaps at finite temperatures we call it *pseudogap*. The opening of such distinct and separated (pseudo)gap regions for the spin and charge degrees at various fillings in μ space is indicative of the corresponding spin-charge separation. The crossover temperatures and phase boundaries for various transitions can be found by monitoring maxima and minima in charge and spin susceptibilities. We define the critical temperatures T_c and T^* in equilibrium as the

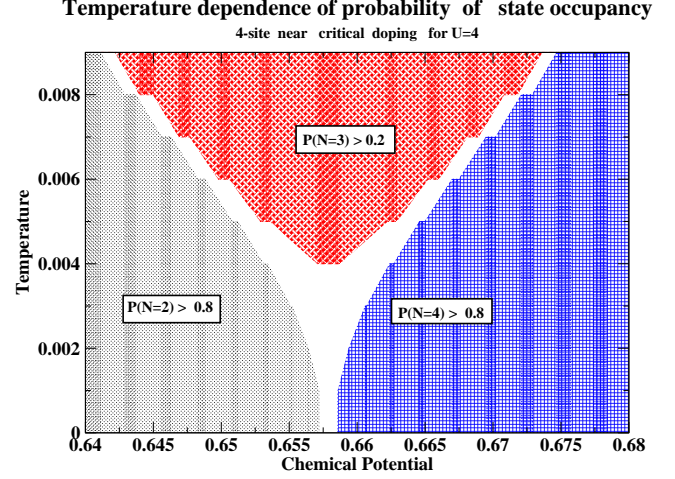


FIG. 1: Thermal occupation probabilities versus μ in the grand canonical ensemble of 4-site clusters in the vicinity of quantum critical point μ_P for $\langle N \rangle \approx 3$ at $U = 4.0$. The phase separation at relatively low temperatures below $T \leq 0.0075$ manifests a significant suppression of $\langle N \rangle = 3$ clusters close to optimal doping $\mu_P = 6.557$. In this area $\langle N \rangle = 2$ and $\langle N \rangle = 4$ clusters share equal weight probabilities, while at higher temperatures $\langle N \rangle \approx 3$ also becomes thermodynamically stable. In equilibrium, the grand canonical value μ_P at optimal doping at $T = 0$ reproduces the result $\mu_P = (\mu_+ + \mu_-)/2$ for the canonical approach.

temperature at which the distances between the charge or spin susceptibility peaks vanish and corresponding pseudogaps disappear (see Sec. V B). Notice that according to the given definition, the energy pseudogaps obtained in the grand canonical method are positive which is a key difference from the canonical gaps.

D. Charge and spin inhomogeneities

The developed grand canonical approach can be applied to understand of the electron fluctuations and the spatial inhomogeneities to model the behavior of the concentrated systems in bipartite and frustrated structures. An ensemble of bipartite clusters at small and moderate U exhibits typical inhomogeneous behavior in its charge distribution. A normalized probability ω_N for the electron distribution in grand canonical ensemble as a function of temperature T for various electron numbers N is the following

$$\omega_N = \sum_n e^{-\frac{E_{nN} - \mu N}{T}} / \sum_{n,N} e^{-\frac{E_{nN} - \mu N}{T}}. \quad (5)$$

The calculated probabilities of electrons in competing configurations are shown in Fig. 1 for the 4-site cluster at $U = 4$. At low temperatures and electron concentration close to μ_P , the clusters with $\langle N \rangle = 2$ and $\langle N \rangle = 4$ have equal probabilities, $\omega_2 = \omega_4 \approx 0.5$. In some circumstances electron configurations in equilibrium can have

close energies for the clusters in contact with a particle reservoir. This picture shows a mixture of ungapped and partially gapped states. As temperature increases, the probability ω_3 of $\langle N \rangle = 3$ clusters with unpaired spin gradually increases, while the probability of finding spin paired, hole-rich and hole-poor clusters decreases.

Qualitatively, the formation of inhomogeneous electron distribution or “stripe” picture can be understood from simple energy considerations (see Sec.II). For a fixed average number of electrons, the charge and spin on each separate cluster in the ensemble can fluctuate. The two configurations close in energy are nearly degenerate, and, as temperature increases, it is energetically favorable to have some clusters with d^{N-1} and another with d^{N+1} , instead of having clusters with d^N electrons. These results, that depend on the cluster geometries, parameter U as well as on the sign of t , can be directly applied to nano and heterostructured materials, which usually contain many independent clusters, weakly interacting with one another with the possibility of having inhomogeneities for a different number of electrons per cluster. At half filling, the antiferromagnetic state has the lowest energy per electron. Therefore, the energy can be minimized upon small doping by segregation of holes into charged clusters with different number of electrons. The embedded antiferromagnetic background with opposite spin pairing provides a spin rigidity (unperturbed) media that allows inhomogeneities to optimize the coherent pair fluctuations across the clusters [24]. The mixture of the closely degenerate ferromagnetic domains can also lead to the stable spatial magnetic inhomogeneities for spin fluctuations. Interestingly, the quantum and thermal fluctuations in the canonical and grand canonical ensembles display “checkerboard” patterns [5], nanophase inhomogeneities [26] and nucleation of pseudogaps driven by temperature seen recently in nanometer and atomic scale measurements [29] in HTSCs above T_s^P [6, 7]. Microscopic spatial inhomogeneities and incoherent pairing pseudogaps in nanophases measured by scanning tunnelling microscopy (STM) correlate remarkably with our predictions using small 4-site and 2×4 nanoclusters [22].

E. Coherent charge and spin pairings

The behavior of such clusters near crossing degeneracies in a quantum coherent phase with minimal spin at low temperatures is somewhat similar to the conventional BCS superconductivity (see Sec. IV A). We found that at rather low temperatures the calculated positive pseudospin gap Δ^s in the grand canonical method can have equal amplitude with a negative charge gap Δ^c derived in canonical method, $\Delta^s = |\Delta^c|$. Such behavior is similar to the existence of a single gap in the conventional BCS state. We call such an opposite spin (singlet) coupling and electron charge pairing as a spin coherent electron pairing in Ref. [24]. However, unlike to the BCS theory, the charge gap differs significantly from the spin pseu-

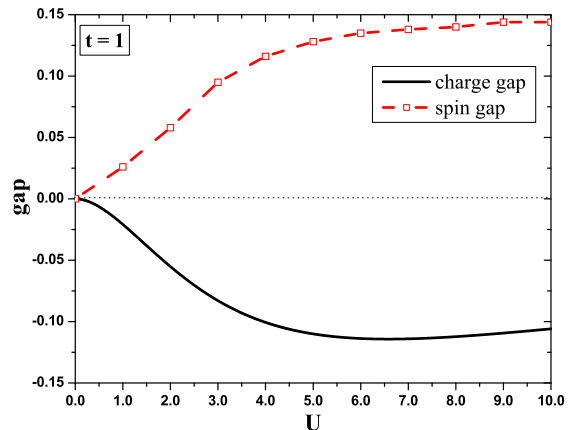


FIG. 2: Charge Δ^c and spin Δ^s gaps versus U in an ensemble of tetrahedrons at $t = 1$, $\langle N \rangle \approx 3$ and $T = 0.001$. Negative charge gap $\Delta^c < 0$ implies charge phase separation, while the positive, opposite spin pairing gap of equal amplitude $\Delta^s \equiv -\Delta^c$ describes Bose condensation of electrons similar to BCS-like coherent pairing with a single (unique) energy gap. This coherent state is analogous to Phase A in 4-site clusters [24]. The spin gap has been calculated using the grand canonical approach.

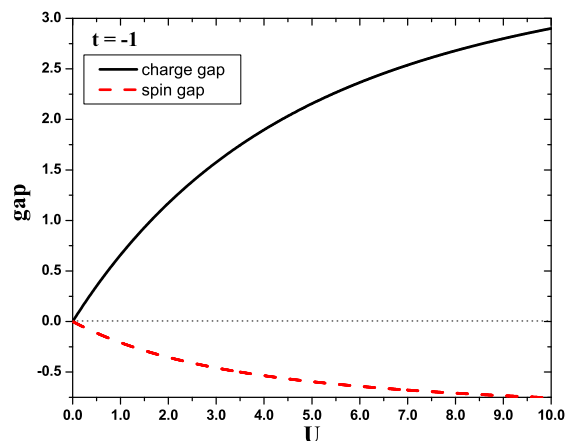


FIG. 3: The charge $\Delta^c > 0$ and parallel (triplet) spin $\Delta^s < 0$ gaps versus U in an ensemble of tetrahedrons at $t = -1$, $\langle N \rangle = 3$ and $T = 0.001$. The positive charge gap for all U describes MH-like insulating behavior analogous to Phase C in 4-site clusters [24]. The negative spin gap ($\Delta^s < 0$), coexisting with the charge pairing gap displays $S = \frac{3}{2}$ Nagaoka saturated ferromagnetism at all $U > 0$ (see Sec. IV B). The charge gap has been calculated using grand canonical approach.

dogap as temperature increases above T_s^P . For example, the vanishing of double peak structure in zero spin susceptibility gives a critical temperature T_s^P , at which the spin pseudogap disappears. The canonical charge gap disappears at higher temperatures, i.e., $\Delta^c(T_c^P) = 0$. The BCS-like coherent behavior and possible superconductivity with condensation of opposite spin pairs occur at rather low temperatures (see Sec. III C), while electron charge pairing can be established at relatively high temperatures, $T_s^P < T_c^P$. The positive spin gap calculated in grand canonical approach implies homogeneous electron (opposite) spin spatial distribution below T_s^P . This picture is consistent with the spatially homogeneous spin pseudogap that opens below $T_c \equiv T_s^P$ in doping dependent STM measurements of $\text{Bi}_2\text{Sr}_2\text{CuO}_{6+x}$ [5]. We also find a close analogy for the coherent electron pairing in clusters with real space singlet pairs in resonance valence bond states or local inter configuration fluctuations in mixed valence states [41, 42, 43, 44, 45, 46].

IV. GROUND STATE PROPERTIES

A. Bipartite clusters

Exact calculations for charge and spin gaps in small clusters in various geometries are important for understanding the electron ground state behavior in bipartite and nonbipartite (frustrated) systems. Below we summarize the results for electron instabilities and phases obtained earlier (see Fig. 1 in Ref. [24]) for square and other bipartite clusters with one hole off half filling at infinitesimal $T \rightarrow 0$. The vanishing of gaps at quantum critical points, $U_c = 4.584$ and $U_F = 18.583$, indicates energy level crossings and electron instabilities in 4-site clusters for charge and spin, respectively. The charge Δ^c and spin Δ^s gaps versus U in an ensemble of square clusters at $\langle N \rangle \approx 3$ exhibit at infinitesimal $T \rightarrow 0$ the following phases; Phase A: Charge and spin pairing gaps of equal amplitude $\Delta^s \equiv \Delta^P = -\Delta^c$ at $U \leq U_c$ describe Bose condensation of electrons similar to BCS-like coherent pairing with a single energy gap; Phase B: Mott-Hubbard like insulator with $\Delta^c > 0$ and gapless $S = \frac{1}{2}$ excitations at $U_c < U < U_F$ describes a spin liquid behavior; Phase C: Parallel (triplet) spin pairing ($\Delta^s < 0$) displays $S = \frac{3}{2}$ the saturated ferromagnetism at $U > U_F$ in Mott-Hubbard insulator for a positive charge gap, $\Delta^c > 0$. Notice, that incoherent opposite spin pairing $|\Delta^s| \neq \Delta^c$, different from the charge pairing at $U < U_c$, suggests spin-charge separation for spin and charge degrees at $U > U_F$.

Square clusters at weak and strong couplings share common important features with 2×4 ladders and other bipartite clusters [36]. Negative gaps describe possible hole binding or parallel spin pairing instabilities. For

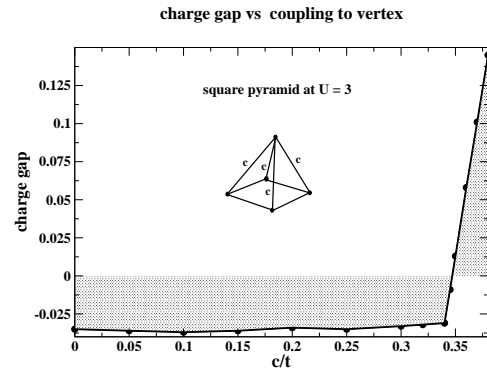


FIG. 4: Charge gap Δ^c versus coupling c between the apex atom and the four base atoms in deformed square pyramid ($t = 1$) for one hole of half filling, $\langle N \rangle = 4$, $U = 3$ and $T = 0.01$. Charge and spin pairing gaps of equal amplitude $\Delta^s \equiv \Delta^P = -\Delta^c$ at $c \leq 0.35$ imply coherent pairing, while $\Delta^c > 0$ and $\Delta^s < 0$ at $c \geq 0.35$ correspond to a ferromagnetic insulator for $S = \frac{1}{2}$.

charge degrees at weak coupling, this gives an indication of phase separation (*i.e.*, *segregation*) into hole-rich (charge neutral) and hole-poor clusters. In contrast, at strong coupling the negative spin pairing gap for parallel spins and positive charge gap reveal ferromagnetic instability in accordance with the Nagaoka theorem. In large bipartite clusters at intermediate U , electrons behave differently from square clusters. For example, in 2×4 ladders we found an oscillatory behavior of charge gap as a function of U [22]. The vanishing of the charge gaps, manifesting the multiple level crossing degeneracies and electronic instabilities in charge and spin sectors, is indicative of possible electron instabilities in bipartite clusters at moderate U .

B. Tetrahedrons

For comparison with small bipartite clusters in Sec. IV A, we consider here a minimal four site nonbipartite structure. A tetrahedron has a topology equivalent to that of a square with the next nearest neighbor coupling ($t' = t$) and may be regarded as a primitive unit of typical frustrated system. Nonbipartite systems, without electron-hole symmetry, exhibit a pairing instability that depends on the sign of t . Notice that sign of t also leads to essential changes in the electronic structure. The tetrahedral clusters show pairing instabilities for charge degrees at $t = 1$ and spin degrees at $t = -1$ that maximizes the amplitudes of negative charge $\Delta^c < 0$ and spin $\Delta^s < 0$ gaps and corresponding condensation temperatures, $T_c^P(\mu)$ and $T_s^F(\mu)$ [47]. The negative gap in the canonical approach displays electron pairing $\Delta^P = |\Delta^c|$ instability for all U . Fig. 3 illustrates the charge and spin gaps at small and moderate U . The negative charge gap in Fig. 2 is indicative of the inhomogeneous charge re-

distribution and phase separation of electron charge into hole-rich (charged) and hole-poor (neutral) cluster configurations [20]. The phase diagram for $t = 1$ is similar to the Phase A in Sec. IV A, but applied for all U values. In contrast, the positive spin gap in the grand canonical approach $\Delta^s > 0$ corresponds to uniform opposite spin distribution in Fig. 2. This BCS-like picture for charge and spin gaps of equal amplitude $\Delta^s \equiv \Delta^P = -\Delta^c$ at $\langle N \rangle \approx 3$, in analogy with the square clusters, will be called coherent pairing (CP) [24]. In equilibrium, the spin singlet background ($\chi_s > 0$) stabilizes phase separation of paired electron charge in a quantum CP phase. Fig. 2 illustrates the charge Δ^c and spin Δ^s gaps in tetrahedral clusters at $\langle N \rangle \approx 3$, $T \rightarrow 0$. The unique gap, $\Delta^s \equiv \Delta^P$ at $T = 0$, in Fig. 2 is consistent with the existence of a single quasiparticle energy gap in the BCS theory for $U < 0$ [25]. Positive spin gap for all U provides pair rigidity in response to a magnetic field and temperature (see Sec. VB). Notice that the coherent pairing exists also at large U where Nagaoka theorem for nonbipartite clusters with specific sign of t can be applied. The stability of minimal spin $S = 0$ (singlet) state in tetrahedron at $t = 1$ is consistent with that of non maximum (unsaturated) spin in Nagaoka problem. Thus our result shows that Nagaoka instability toward spin flip at large U in frustrated lattices with $t = 1$ can be associated with the BCS-like coherent pairing applied for general U .

The negative spin gap Δ^s in Fig. 3 is shown for canonical energy differences between $S = \frac{3}{2}$ and $S = \frac{1}{2}$ configurations. Correspondingly, the positive charge gap $\Delta^c > 0$ in a stable MH-like state is derived using grand canonical energies [20]. As in bipartite square clusters, the grand canonical positive charge gap $\Delta^c > 0$ is different (incoherent) from the parallel spin pairing gap, $\Delta^s < 0$. Thus the phase diagram for $t = -1$ with $\Delta^c \neq -\Delta^s$ is similar to the Phase C in Sec. IV A, but applied for all U values in the phase diagram. The negative spin gap for all couplings implies parallel spin pairing and Nagaoka-like saturated ferromagnetism with maximum spin in the entire range of U . Spin-charge separation is considered to be one of the key properties of the correlated electrons that distinguishes $t = -1$ from $t = 1$. Such behavior at $t = -1$ is accompanied by spin-charge separation and formation of the magnetic (spatial) inhomogeneities or domain structures [20] in a wide range of parameters.

C. Square pyramids

From the early days of high-temperature superconductivity, the idea of a possible role of apical sites in p-type superconductors has been controversial. The oxygen atom position at the apex of pyramidal crystalline structure can be altered through the addition of impurities and can be relocated to a lower or sideways position, thus changing the electron interactions or coupling strength c between apex and the planar atoms. There is no significant influence of localized electron charge of

apical site on electron pairing and possible superconductivity in CuO_2 planes in $\text{Bi}_2\text{Sr}_2\text{CaCu}_2\text{O}_{8+\delta}$. When excess apex does not exist, *i.e.*, $\delta = 0$, this system is an insulator. However, when excess apex oxygen is introduced, hole carriers are supplied into CuO_2 planes and the material shows superconductivity [48]. Here we try to draw a closer connection to HTSCs perovskites and consider an ensemble of square pyramids of octahedral structure.

Fig. 4 shows the charge gap at fixed $U = 3$ and $\langle N \rangle \approx 4$ under the variation of the coupling term c between the plane and the apex atoms. This picture gives surprisingly plausible evidence for understanding the detrimental role of excess electron on charge pairing for possible distortions of pyramidal crystalline structure in perovskites. In Fig. 4, the strong distortion of the pyramid structure for $c = 0$ (with reduced coordination number) reproduces a charge pairing gap in planar square geometries. At $\langle N \rangle \approx 4$, the electron is localized and there is no charge transfer from apex atom in an ensemble of pyramid clusters at $c = 0$. The negative charge gap, identical to the spin gap, exists only for $c \leq c_0$, where $c_0 = 0.35$ is a quantum critical point for level crossing degeneracy. Calculated electron distribution, as a function of c , shows that electron charge residing on the apical site does not contribute to the pairing whenever c is less than c_0 . The coupling in the pyramid structure at $c < c_0$ for $\langle N \rangle \approx 4$ leads to charge pairing instability with negative charge and positive spin gaps of equal amplitude as seen in square clusters at $\langle N \rangle \approx 3$ in Sec. IV A. In contrast, at $c > c_0$, the induced charge gap driven by c change leads to electron hole pairing and a transition into insulating Mott-Hubbard (MH) behavior with $\Delta^c > 0$. The apex atom, coupled to square-planar geometry, have shown to have a detrimental affect on the negative charge and positive spin gaps, which are favorable to forming a Bose condensate in the region of instability. We found a coherent pairing in the phase diagram with one hole off half filling also in the ensemble of octahedron clusters (perovskite systems) in Ref. [49]. There is also shown that octahedron threaded by magnetic flux in hole-rich regions can get trapped in stable minima at half integral units of the magnetic quantum flux. Such approach can be applied to understand the detrimental effect of the transverse magnetic field on electron charge and opposite spin pairings for possible superconductivity in HTSCs in planar face centered square (fcs) geometry [24].

V. PHASE T- μ DIAGRAM

A. Tetrahedrons at large U and $t = 1$

The charge and spin susceptibility peaks in clusters, reminiscent of the singularities in infinite systems, display an extremely rich phase diagram at finite tempera-

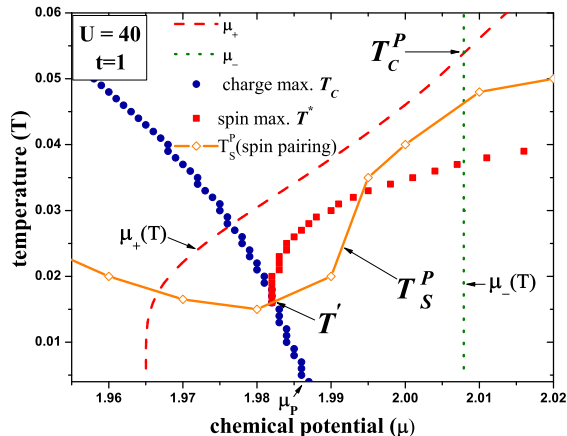


FIG. 5: The T - μ phase diagram of tetrahedrons without electron-hole symmetry at optimally doped $\langle N \rangle \approx 3$ regime near $\mu_P = 1.998$ at $U = 40$ and $t = 1$ illustrates the condensation of electron charge and onset of phase separation for charge degrees below T_c^P . The incoherent phase of preformed pairs with unpaired opposite spins exists above T_s^P . Below T_s^P , the paired spin and charge coexist in a coherent pairing phase. The charge and spin susceptibility peaks, denoted by T^* and T_c , define pseudogap regions calculated in the grand canonical ensemble, while phase boundaries $\mu_+(T)$ and $\mu_-(T)$ are evaluated in the canonical ensemble. The spin pseudogap region exists for $T_s^P < T < T'$. Charge and spin peaks reconcile at $T \sim T'$, while χ^c peak below T_s^P signifies metallic (charge) liquid (see inset for square cluster in Ref. [22]).

tures. The realization of a high transition temperature, T_c , in clusters and bulk systems depends on the interaction strength U , doping, and the detailed nature of the crystal structure (sign and amplitude of t). As exemplified here, the critical temperatures for various pairing instabilities in frustrated clusters also strongly depend on the sign of the hopping (t) term. Fig. 5 for $t = 1$ illustrates a number of nanophases, defined in Refs. [20, 22], for the tetrahedron at large $U = 40$, found earlier in tetrahedron and bipartite 2×2 and 2×4 clusters at moderate $U = 4$ values [24]. This diagram captures the essential electron charge and spin pairing instabilities at finite temperatures. The curve $\mu_+(T)$ below T_c^P signifies the onset of charge pair condensation. The calculated susceptibility peaks in Fig. 5 correspond to the pseudogap crossover temperature T^* . As temperature is lowered below T^* , a spin pseudogap is opened up first, as seen in NMR experiments [22], followed by the gradual disappearance of the spin excitations, consistent with the suppression of low-energy excitations in the HTSCs probed by STM and ARPES [3, 4, 5, 6, 7]. In contrast, the local charge gap, Δ^c , evolves smoothly as temperature decreases below T_c^P . The opposite spin CP phase, with fully gapped collective excitations, begins to form at $T \leq T_s^P$ and spin pairing rigidity gradually grows upon

lowering of the temperature. As temperature decreases both charge and spin pseudogaps emerge into one gap at zero temperature. Therefore, at sufficiently low temperatures, this leads to the BCS-like coherent coupling of electron charge to bosonic excitations (see Sec. IV B). However, the spin gap is more fragile and as temperature increases it vanishes at T_s^P , while charge pseudogap survives until T_c^P .

The charge inhomogeneities [1, 2] in hole-rich and charge neutral *spinodal* regions between μ_+ and μ_- are similar to those found in the ensemble of squares and resemble important features seen in the HTSCs. Pairing and transfer of holes is a consequence of the existence of an inhomogeneous background. In the absence of direct contact between clusters, the inhomogeneities in the grand canonical approach are establishing a transfer of paired electrons via this (thermal) bath media. Fig. 5 shows the presence of bosonic modes below $\mu_+(T)$ and T_s^P for paired electron charge and opposite spin respectively. This picture suggests condensation of electron charge and spin at various crossover temperatures while condensation in the BCS theory occurs at a unique T_c value. This result suggests that thermal excitations in the exact solution are not quasiparticle-like renormalized electrons, as in the BCS theory, but collective paired charge and coupled opposite spins [24].

The coherent pairing of holes here is a consequence of the existence of homogeneous opposite spin pairing background, consistent with the STM measurements [29]. This led us to conclude that T_s^P can be relevant to the superconducting condensation temperature T_c in the HTSCs. In the absence of spin pairing above T_s^P , the pair fluctuations between the two lowest energy states becomes incoherent. The temperature driven spin-charge separation above T_s^P resembles an incoherent pairing (IP) phase seen in the HTSCs [2, 3, 4, 5, 6]. The charged pairs without spin rigidity above T_s^P , instead of becoming superconducting, coexist in a nonuniform, charge degenerate IP state similar to a ferroelectric phase [25]. The unpaired weak moment, induced by a field above T_s^P , agrees with the observation of competing dormant magnetic states in the HTSCs [4]. The coinciding χ^s and χ^c peaks in the vicinity of critical temperature T' show full reconciliation of charge and spin degrees seen in the HTSCs above T_c . However, in both channels the charge and spin pseudogaps behave differently or independently. Indeed, we find that the variation of the spin pairing gap with temperature does not cause a change in the charge pairing gap. In the absence of electron-hole symmetry in the tetrahedrons, the reentrant phenomenon can be observed at low temperatures [24]. In Fig. 5, as temperature increases near optimal doping $\mu \leq \mu_P$, clusters undergo a transition from a CP phase to a MH-like behavior. Notice that the charge and spin pairing do not disappear in the underdoped regime for $\mu \geq \mu_P$ but are governed predominantly by the physics of antiferromagnets at half filling. In contrast, in the overdoped regime at low temperatures, the charge pairing pseudogap gradually approaches the

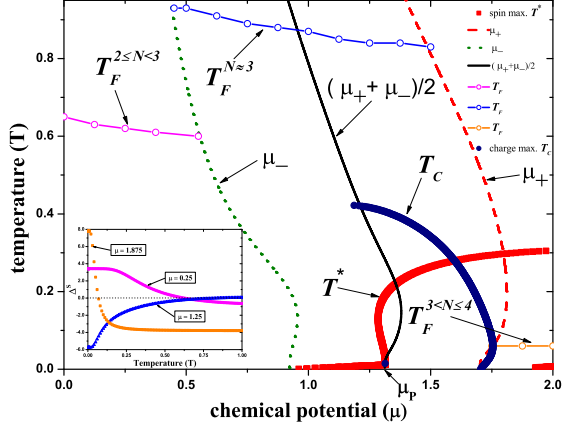


FIG. 6: The T - μ phase diagram of square clusters near optimally doped $\langle N \rangle \approx 3$ regime at $U = 40$ illustrates the condensation of electron spin and onset of phase separation for spin degrees below T_F^N for various N regions in μ space. The charge and spin susceptibility peaks, denoted by T_c and T^* , define corresponding pseudogap regions calculated in the grand canonical ensemble, while boundaries for stable ferromagnetic transitions $\mu_+(T)$ and $\mu_-(T)$ are evaluated in the canonical ensemble. In equilibrium, the grand canonical value μ_P at optimal doping $\langle N \rangle = 3$ at $T = 0$ reproduces the result $\mu_P = (\mu_+ + \mu_-)/2$ for canonical approach. The inset shows variation of canonical spin gap Δ^s versus temperature for various values of μ .

spin pseudogap as in the conventional BCS theory.

Our exact calculations of phase diagrams in various bipartite and nonbipartite clusters provide strong evidence for the existence of a narrow, homogeneous (pseudo)gap Δ^s that vanishes near T_s^P , coexisting with inhomogeneous, weakly temperature dependent broad gap Δ^c , which disappears at higher temperatures $T_c^P > T_s^P$. These phase diagrams display coherent and incoherent pairing (pseudo)gaps and possible superconductivity in agreement with the recent STM measurements in HTSCs [1, 2, 3, 4, 5, 6, 7].

B. Bipartite clusters at large U

As for the cuprates, the bipartite clusters are useful for understanding the magnetic behavior and instabilities in manganites. The phase diagram in Fig. 6 for square clusters at $U = 40$, quite similar to other bipartite clusters at large U limit [21], displays characteristic features of manganites with strong electron correlations. In the ground state, the cluster at $\langle N \rangle = 3$ exhibits ferromagnetism in agreement with the Nagaoka theorem [36]. However, we observe saturated ferromagnetism, $S = \frac{3}{2}$ spin state for $\langle N \rangle \approx 3$ clusters with one

hole off half filling also at finite temperatures. The curve below $T_F^{N \approx 3}$ signifies the onset of spontaneous magnetization with $S = \frac{3}{2}$ for parallel spin condensation. The positive charge gap ($\Delta^c = 0.7787$) for electron-hole (exciton) pairing manifests MH-like insulating behavior. In contrast, clusters show the minimum spin $S = 0$ antiferromagnetism at $\langle N \rangle \approx 2$ and $\langle N \rangle \approx 4$ in the ground state and at finite temperatures. The inset in Fig. 6 displays the variation of spin gap for various regions. At $\mu = 1.35$ the negative spin gap for $\langle N \rangle \approx 3$ approaches zero as $T \rightarrow T_F^{N \approx 3}$. Thus the region above $T_F^{N \approx 3}$ describes a paramagnetic phase with zero spin gap for unpaired spins. In contrast, the positive spin gap in high doped regime at $\mu = 0.25$ changes its sign at temperatures above $T_F^{2 \leq N < 3}$. This picture describes a transition driven by temperature from antiferromagnetism into ferromagnetism with $S = 1$. At half filling, a MH-like antiferromagnetism is stable at very low temperatures and unsaturated ferromagnetic state with $S = 1$ becomes more stable at higher temperatures, $T \geq T_F^{3 < N \leq 4}$. However, $T_F^{3 < N \leq 4} \rightarrow 0$ as $U \rightarrow \infty$ and unsaturated ferromagnetism with $S = 1$ at half filling can be stabilized at infinitesimal temperatures. The well separated charge and spin susceptibility curves in the entire parameter range near $\langle N \rangle \approx 3$ show spin-charge separation and decoupling of charge and spin degrees. The susceptibility peak at T^* for $\langle N \rangle \approx 3$ in Fig. 6 displays a spin liquid behavior in the overdoped region for $\mu \leq \mu_P$, while well developed negative spin gap in underdoped for $\mu > \mu_P$ regions at low temperatures describes a ferromagnetic insulator. In Fig. 6, the region of metallic-like behavior is manifested by the charge susceptibility peaks along the T_c curve.

Phase diagram with μ dependent locally inhomogeneous, $\Delta^s < 0$, and homogeneous, $\Delta^s > 0$, spin structures at low temperatures, coexisting with charge ordered homogeneous Mott-Hubbard like gap $\Delta^c > 0$ displays spin-charge separation and characteristic features of the CMR-manganite $\text{La}_{1-x}\text{Ca}_x\text{MnO}_3$ and related materials with alternating insulating ferromagnetic and charge ordered antiferromagnetic regions [51].

VI. CONCLUSION

We have studied the dependence of the ground state and thermal properties in the repulsive Hubbard model on cluster size, geometry, electron number and interaction strength to understand the inhomogeneous superconducting elements and stripes. The inhomogeneities found in exact calculations of clusters are promising for the description of geometric stripes with alternating superconducting and antiferromagnetic regions in high- T_c cuprates and magnetic domain structures in manganites. Spatial electron inhomogeneities capture the magnetic and pairing instabilities in clusters and respective bulk materials. The principal conclusion is that the exact solution for optimal inhomogeneities mimicked in small clusters can target essential features relevant to exist-

ing inhomogeneities in nanostructured materials on a nanoscale level. We found charge and spin gaps of equal amplitude in the ground state similar to the coherent pairing in conventional BCS theory. However, separate Bose condensation of electron charge and spin degrees with two consecutive transition temperatures into coherent pairing suggests a mechanism different from the prediction of the BCS coherent behavior with a unique critical temperature. This picture is also consistent with the existence of two different energy scales for electron charge and spin pairing condensation temperatures in the HTSCs [1, 2, 3, 4, 5, 6].

The electronic instabilities in various geometries and in a wide range of U and temperatures will be useful for the prediction of coherent and incoherent electron pairings, ferroelectricity [9, 25] and possible superconductivity in nanoparticles, doped cuprates, etc. In contrast to bipartite clusters, the exact solution for the tetrahedron depends on the sign of t and shows relatively weak dependence on U . For example, the tetrahedron exhibits similar features at $U = 4$ and $U = 40$ whenever $t = 1$. On other hand, the behavior of the tetrahedron for $t = -1$ strongly differs from that of $t = 1$. These results for frustrated clusters show that the properties are more sensitive to the change of the sign of the hopping term rather than the U parameter. This fact can explain why itinerant ferromagnetism can occur even at relatively weak interactions in frustrated systems. Our findings at small, moderate and large U carry a wealth of infor-

mation regarding phase separation, ferromagnetism and Nagaoka instabilities in bipartite and frustrated nanostructures in manganites/CMR materials at finite temperatures. These exact results allow us to understand the origin of level crossings, spin-charge separation, reconciliation and full Bose condensation [52]. The obtained phase diagrams provide novel insight into electron condensation, magnetism, ferroelectricity at finite temperatures and display a number of inhomogeneous, coherent and incoherent nanophases seen recently by STM and ARPES in numerous nanomaterials, assembled nanoclusters and ultra-cold fermionic atoms [10, 53].

Finally, we conclude that the use of the chemical potential and the departure from zero degree singularities in the canonical and grand canonical ensembles are essential for understanding the important thermal properties and physics of phase separation instabilities and inhomogeneities at nanoscale level. The article currently in progress is aimed to study the stability of pairing correlations and magnetism in the presence of transverse magnetic field [49]. It will be shown that magnetic flux tube inside the octahedral cluster can get trapped in stable minima at half integral units of the flux quantum in hole-rich regions.

We thank Daniil Khomskii and Valery Pokrovsky for helpful discussions. This research was supported in part by U.S. Department of Energy under Contract No. DE-AC02-98CH10886.

-
- [1] Y. Kohsaka *et al.*, Science **315** (2007) 1380.
 - [2] T. Valla *et al.*, Science **314** (2006) 1914.
 - [3] A. C. Bódi, R. Laiho, and E. Lähderanta, Physica C **411** (2004) 107.
 - [4] H. E. Mohottala *et al.*, Nature Materials **5** (2006) 377.
 - [5] M. C. Boyer, Nat. Phys. **3** (2007) 802.
 - [6] K. K. Gomes *et al.*, Nature **447** (2007) 569.
 - [7] A. N. Pasupathy *et al.*, Science **320** (2008) 196.
 - [8] R. E. Cohen, Nature **358** (2005) 136.
 - [9] R. Moro, S. Yin, X. Xu, and W. A. de Heer, Phys. Rev. Lett. **93** (2004) 086803; X. Xu, S. Yin, R. Moro, and W. A. de Heer, **95**, (2005) 237209.
 - [10] S. Y. Wang, J. Z. Yu, H. Mizuseki, Q. Sun, C. Y. Wang, and Y. Kawazoe, Phys. Rev. B **70** (2004) 165413.
 - [11] C. Yang, A. N. Kocharian, and Y. L. Chiang, J. Phys.: Condens. Matter **B12** (2000) 7433.
 - [12] H. Shiba and P. A. Pincus, Phys. Rev. B **5** (1972) 1966.
 - [13] L. M. Falicov and R. H. Victora, Phys. Rev. B **30** (1984) 1695.
 - [14] L. Tan and J. Calaway, Phys. Rev. B **46**, 5499 (1992); *ibid* **35** (1987) 8723.
 - [15] R. Schumann, Ann. Phys. **11** (2002) 49; *ibid* **17** (2008) 221.
 - [16] J. H. Hirsch, Phys. Rev. B **67** (2003) 035103.
 - [17] S. Belluci, M. Cini, P. Onorato, and E. Perfetto, J. Phys.: Condens. Matter **18**, S2115 (2006); W.-F. Tsai and S.A. Kivelson, Phys. Rev. B **73**, 214510 (2006); S.R. White, S. Chakravarty, M.P. Gelfand, and S.A. Kivelson, *ibid* **B45**, 5062 (1992); R.M. Fye, M.J. Martins, and R.T. Scalettar, *ibid* **42**, R6809 (1990); N.E. Bickers, D.J. Scalapino, and R.T. Scalettar, Int. J. Mod. Phys. B **1**, 687 (1987).
 - [18] A. N. Kocharian, G. W. Fernando, K. Palandage, and J. W. Davenport, arXiv:cond-mat.str-el/0510609v1 (2005) (unpublished).
 - [19] A. N. Kocharian, G. W. Fernando, K. Palandage and J. W. Davenport, J. Magn. Magn. Mater. **300** (2006) e585.
 - [20] A. N. Kocharian, G. W. Fernando, K. Palandage, and J. W. Davenport, Phys. Rev. B **74** (2006) 024511.
 - [21] A. N. Kocharian, G. W. Fernando, K. Palandage, and J. W. Davenport, Phys. Lett. A **364** (2007) 57.
 - [22] G. W. Fernando, A. N. Kocharian, K. Palandage, Tun Wang, and J. W. Davenport, Phys. Rev. B **75** (2007) 085109.
 - [23] K. Palandage, G. W. Fernando, A. N. Kocharian and J. W. Davenport, J. Comput.-Aided. Mater. Des. **14** (2007) 103.
 - [24] A. N. Kocharian, G. W. Fernando, K. Palandage, and J. W. Davenport, Phys. Rev. B **78** (2008) 075431.
 - [25] A. N. Kocharian, G. W. Fernando, K. Palandage, and J. W. Davenport, ISPM Seattle'08 conference proceedings, Ultramicroscopy, to be published (2009).
 - [26] J. M. Tranquada *et al.*, Nature (London) **375** (1995) 561.
 - [27] E. Arrigoni, and S. A. Kivelson, Phys. Rev. B **68** (2003) 180503.
 - [28] J. Eroles, G. Ortiz, A. V. Balatsky, A. R. Bishop, In-

- ter. J. Mod. Phys. **15** (2001) 2833.
- [29] W. D. Wise *et al.*, Nature Physics **4**, 696 (2008).
 - [30] V. J. Emery, S. A. Kivelson, and H. Q. Lin, Phys. Rev. Lett. **64** (1990) 475.
 - [31] E. Dagotto, Science **309** (2005) 257. Phys. Rev. Lett. **64** (1990) 475.
 - [32] E. L. Nagaev, Physics - Uspechi **39** (1996) 781.
 - [33] E. L. Nagaev, Physica B **230-232** (1997) 816.
 - [34] V. Kiryukhin, T. Y. Koo, H. Ishibashi, J. P. Hill, and S-W. Cheong, Phys. Rev. B **67** (2003) 064421.
 - [35] L. N. Bulaevskii, C. D. Batista, M. V. Mostovoy, D. I. Khomskii, Phys. Rev. B **78** (2008) 024402.
 - [36] Y. Nagaoka, Phys. Rev. **147** (1966) 392.
 - [37] J. B. Sokoloff, Phys. Rev. B **3** (1971) 3826.
 - [38] A. N. Kocharian, C. Yang, Y. L. Chiang, and T. Y. Chou, Inter. J. Mod. Phys. B **17** (2003) 5749.
 - [39] W. P. Halperin, Rev. Mod. Phys. **58** (1986) 533.
 - [40] C. Herring, "Exchange Interactions Among Itinerant Electrons", in Magnetism Vol IV, G.T. Rado and H. Suhl eds., Academic Press, New York, 1966.
 - [41] P W. Anderson, Mater. Res. Bul. **8** (1973) 153.
 - [42] P. Fazekas and P W. Anderson, Philos. Mag. **30** (1974) 432.
 - [43] P W. Anderson, Science **235** (1967) 1196.
 - [44] F. W. J. Hekking *et al.*, Phys. Rev. Lett. **70** (1993) 4138.
 - [45] J. Koch, M. E. Raikh, and F. von Oppen, Phys. Rev. Lett. **90** (2006) 056803.
 - [46] A. N. Kocharian and Khomskii, [Zh. Eksp. Teor. Fiz., **71** (1976) 767] Sov. Phys. JETP **44** (1976) 404.
 - [47] I. A. Sergienko and S. H. Curnoe, Phys. Rev. B **70** (2004) 144522.
 - [48] H. Kamimura, H. Ushio, S. Matsuno, T. Hamada, Theory of Copper Oxide Superconductors, Chapter VII: Electronic Structure of a CuO₅ Pyramid in Bi₂Sr₂CaCu₂O_{8+d}, Springer Berlin Heidelberg, pp 51-53 (2005).
 - [49] G. W. Fernando, K. Palandage, A. N. Kocharian, and J. W. Davenport, submitted to Phys. Rev. B (2009).
 - [50] Y. Murakami *et al.*, Nature **423** (2003) 965.
 - [51] New Trends in the Characterization of CMR-Manganites and Related Materials, edited by K. Baerner Research Signpost, Trivandrum (2005).
 - [52] R. Friedberg, T. D. Lee, and H. C. Ren, Phys. Rev. B **50** (1994) 10190.
 - [53] J. K. Chin *et al.*, Nature **443** (2006) 961.